On the Mechanism of Isotope Exchange Kinetics of Single Protons in Bovine Pancreatic Trypsin Inhibitor†

Bruce D. Hilton and Clare K. Woodward*

ABSTRACT: The hydrogen isotope exchange kinetics of the slowest exchanging proton resonances in the bovine pancreatic trypsin inhibitor nuclear magnetic resonance spectrum were measured from pH 1 to 12, 33–68 °C. The pH dependence and the apparent activation energy for each proton vary with temperature. The kinetics for each proton are explained by a model in which exchange is governed by two discrete conformational processes that differ in temperature dependence. One process is related to thermal unfolding, and kinetics for exchange by this pathway are of high activation energy, ~60 kcal/mol, and about half-order in OH^- ion. The second is a dynamical process of the folded conformation, and kinetics for exchange by this process give an activation energy of 20–35 kcal/mol with variable pH dependence approaching first order in catalyst ion. Since the chemical exchange step has an activation energy of ≃20 kcal/mol, the enthalpies of the two conformational processes are ≃40 and 0–15 kcal/mol, respectively. The model is simple, has a precedent in the hydrogen-exchange literature, and predicts the complex features of the pH and temperature dependence of the single proton exchange rates, including the data of Richarz et al. [Richarz, P., Sehr, P., Wagner, G., & Wuthrich, K. (1979) *J. Mol. Biol. 130*, 19] and Wagner & Wuthrich [Wagner, G., & Wuthrich, K. (1979) *J. Mol. Biol. 130*, 31]. For the two slowest exchanging protons, the rates at 51 °C show a pH-independent plateau between pH 8.4 and 9.6. In the context of our model, comparison with data for the same resonances at 45 °C suggests that the high activation energy conformational process is rate limiting at pH >8.4, 51 °C, and the rate of exposure to solvent is equal to the observed exchange rate, 5×10^{-2} h^{-1}.

There is increasing evidence that the internal structure of the folded conformation of globular proteins is dynamic, with interior atoms undergoing rapid fluctuations on the order of tenths of angstroms in the vicinity of the time-average X-ray structure (McCammon et al., 1977, 1979; Woodward & Hilton, 1979; Weber, 1975; Gurd & Rothgeb, 1979; Wagner & Wuthrich, 1978; Richards, 1979; Frauenfelder, 1978; Jelinski & Torchia, 1979; Munro et al., 1979). The hydrogen isotope exchange kinetics of backbone amide protons in native proteins monitor the accessibility of the closely packed protein matrix to solvent and consequently are a measure of the long-time internal motions in the solution structure. The observation that most buried amide protons in native proteins have slow, but finite, isotope exchange rates was for over a decade the main experimental indication of internal motions in unperturbed proteins (Linderstrøm-Lang, 1958; Hvidt & Neilsen, 1966; Englander et al., 1972).

Briefly, for total hydrogen isotope exchange of globular proteins, the following are known: 85–90% of the amide protons exchange from the folded conformation with no contribution from unfolding (Woodward & Rosenberg, 1971a; Ellis et al., 1975); under certain conditions of pH and temperature the major unfolding transition may contribute to or dominate the observed exchange kinetics (Woodward et al., 1975a; Ellis et al., 1975; Tsuboi & Nakanishi, 1979); native proteins exchange with a distribution of exchange rates 4–8 orders of magnitude broader than the distribution of rates for the equivalent unfolded peptide, with the fastest rates equivalent to those of the unfolded protein (Woodward & Rosenberg, 1970, 1971b; Molday et al., 1972; Lebedev et al., 1976); the activation energy for the conformational contribution to exchange is typically 0–15 kcal/mol (Woodward & Rosenberg, 1971a; Ellis et al., 1975; Woodward & Ellis, 1975; Woodward, 1977); denaturing cosolvents, at concentrations below those inducing unfolding, do not affect hydrogen exchange rates from the native conformation (Woodward et al., 1975b; Ellis et al., 1975); exchangeable protons at the interface of a dimer exchange with a pH and temperature dependence normal for buried protons in globular proteins and without apparent contribution of dimer dissociation (Woodward, 1977); the activation volume is markedly pressure dependent for folded proteins but not for unfolded proteins (Carter et al., 1978); ligands often decrease exchange rates of native proteins, but in some instances ligands increase exchange rates or have no effect [see references in Woodward & Hilton (1979)].

For the protein process governing solvent accessibility in the solution structure of proteins, two limiting types of models have been proposed. In one, water molecules and catalyst ions penetrate the buried regions of the protein via small-amplitude motions, each too small to accommodate solvent molecules or ions but which may collect as holes or pathways for solvent species into the protein matrix where exchange occurs (Woodward & Rosenberg, 1971a; Ellis et al., 1975; Woodward, 1977). Lumry and Rosenberg have suggested a more specific mechanism of internal fluctuations involving the redistribution of mobile defects, or void volume cavities created primarily by rearrangements of hydrogen bonds, that allows the diffusion of one hydroxyl ion or hydrogen ion in combination with at least one water molecule (Lumry & Rosenberg, 1975; Lumry, 1978). The second type of model involves larger amplitude motions that expose a region of the protein to bulk solvent where exchange takes place. Motions suggested are unspecified open–close reactions (Hvidt & Neilsen, 1966; Hvidt, 1973), local reversible unfolding (Englander, 1975; Schreier & Baldwin, 1977), local unfolding of a segment of secondary structure in which several broken hydrogen bonds, distributed randomly over the molecule, are statistically localized in adjacent peptides of the same secondary structural element (Nakanishi et al., 1973; Tsuboi & Nakanishi, 1979), and motions of hydrophobic domains relative to each other by open–close transitions of hydrogen-bonded secondary

† From the Department of Biochemistry, University of Minnesota, St. Paul, Minnesota 55108. *Received August 7, 1979.* This work was supported by National Institutes of Health Grant GM-26242 and by the University of Minnesota Graduate School.

0006-2960/79/0418-5834$01.00/0

structure (Wagner & Wuthrich, 1978; Wuthrich et al., 1978a). The evidence cited in support of each type has been reviewed (Woodward & Hilton, 1979; Gurd & Rothgeb, 1979; Englander & Englander, 1978; McCammon & Karplus, 1979).

In crystals of myoglobin, ≃95% of the peptide NH protons exchange with deuterium after perfusion with deuterium solvent (Schoenborn et al., 1978). Also, recent studies of the temperature dependence of the myoglobin crystal structure indicate that the interior atoms fluctuate in the crystal (Frauenfelder et al., 1979). It is possible that the types of small atomic displacements observed in the temperature (Frauenfelder et al., 1979) and ligand (Deatherage et al., 1976; Huber et al., 1974) perturbation of protein crystal structure provide solvent accessibility for NH protons in the crystalline state and further that these motions are related to the fluctuations that expose buried atoms in the solution structure to solvent (Woodward & Hilton, 1979).

The interpretation of total hydrogen exchange in proteins has been limited by the lack of adequate methods for the analysis of the complicated kinetics, although promising advances have been made by the introduction of a distribution function constructed from the reverse Laplace transform of the total exchange kinetics (Knox & Rosenberg, 1980). To simplify the analysis of hydrogen exchange kinetics in solution, we have turned to the study of single proton exchange rates by NMR spectroscopy (Hilton & Woodward, 1978).

Hydrogen–deuterium exchange rates of single atoms are obtained from the decay rates of the ^1H NMR signal in deuterium solvent. Bovine pancreatic trypsin inhibitor (BPTI) is an ideal model for the initial studies of single proton exchange by NMR spectroscopy. It is small, molecular weight 6500, and stable over an unusually broad range of pH and temperature. The high-resolution X-ray crystal structure is known (Huber et al., 1971), and it has been the subject of extensive NMR spectroscopic characterization (Karplus et al., 1973; Marinetti et al., 1976; Wagner et al., 1976; Wagner & Wuthrich, 1978; Richarz & Wuthrich, 1978; Wuthrich et al., 1978b; Wuthrich & Wagner, 1979). BPTI is also the model protein used for dynamical calculations of small amplitude motions in proteins by Karplus, McCammon, and co-workers (Gelin & Karplus, 1975, 1977; McCammon et al., 1977, 1979).

In this paper we have extended our previous high-temperature studies of the slowest exchanging protons in BPTI (Hilton & Woodward, 1978). These are conveniently observed as they are shifted downfield and well resolved from the aromatic envelope. The exchange rates of these protons at lower temperatures have recently been reported (Wuthrich & Wagner, 1979; Richarz et al., 1979). These resonances have been assigned to individual atoms (Dubs et al., 1979). Our present results indicate that there are two discrete types of dynamic processes having markedly different activation energies that account for the accessibility of each slowly exchanging proton in the temperature range 22–68 °C, pH 1–12.

Experimental Section

Bovine pancreatic trypsin inhibitor (BPTI) (Novo Industries, Denmark) was dialyzed against deionized water at neutral pH to remove low molecular weight impurities and stored as the lyophilized powder. D_2O (99.8%, Stohler) was treated by extraction with dithiocarbazone in carbon tetrachloride to remove metals (Hilton & Bryant, 1976). Sodium 3-(trimethylsilyl)propionate-*2,2,3,3-d*$_4$ (TSP) (Merck Sharpe & Dohme) was used without further purification.

BPTI buffers and solvents were preequilibrated to 25 °C for at least 1 h, and then 20 mg of protein was added directly to 1 mL of D_2O, 0.3 M in KCl, and the pH was adjusted with DCl and/or KOD. Spectra were obtained with a Bruker HX-270 spectrometer equipped with temperature control. Temperatures were calibrated by using ethylene glycol (Piccinni-Leopardi et al., 1976). In Hilton & Woodward (1978) the data are reported in terms of pD, taken as the pH meter reading plus 0.4, the correction for the potential change in the glass electrode in deuterium solvent (Glasoe & Long, 1960). Here, the pH meter reading in 98% deuterium solution, pH*, is reported without correction since it appears that the equilibrium isotope effect compensates for the effect of the deuterium on the glass electrode (Bradbury & Brown, 1973).

NMR spectra were obtained in the Fourier transform mode by using an internal deuterium lock. The HOD resonance was selectively saturated by using 33 dB of decoupler power. From 1500 to 10 800 scans were accumulated for individual spectra, continuously recorded during an exchange experiment with the sample remaining in the spectrometer.

Resonance intensities were obtained as in the previous report (Hilton & Woodward, 1978). Errors in rates were estimated to be within 10% except where indicated. The error in the activation energies from the linear portion of the temperature dependence was ±10% based on a linear least-squares fit.

Results

We have previously reported the hydrogen isotope exchange rates of the downfield resonances of BPTI at 68 °C (Hilton & Woodward, 1978). The high temperature was chosen so that the exchange could be conveniently followed over the pH range that spans the pH of minimum rate, pH_{min}. BPTI is unusually stable and at 68 °C is >20 °C below thermal unfolding detectable by NMR (Masson & Wuthrich, 1973; Wagner et al., 1976). As the exchange is acid/base catalyzed and has a high activation energy, the temperature was lowered in order to bring the exchange rates at pH* >7 into the observation window, 1–48 h.

Exchange rates from pH* 7 to 10 were determined at 51.3 and 33 °C (Figure 1). Resonances are numbered as in Hilton & Woodward (1978). The data at 68 °C reported earlier along with new data at pH* 1.1, 1.4, 1.9, and 2.3 are also shown in Figure 1. For three of the protons, the pH–rate profiles for the predicted chemical-exchange step are shown by dashed lines; these are calculated for each proton from the empirical nearest-neighbor rules of Molday et al. (1972), based on the assignments of Dubs et al. (1979). The assignments of Dubs et al. (1979) are indicated in parentheses after the resonance number.

As noted earlier (Hilton & Woodward, 1978) for these protons at 68 °C, the pH_{min} is higher than for unfolded peptides and the base-catalyzed exchange rates show less than first-order dependence on OH^- ion. The latter is indicated by the fact that $\Delta(\log k)/\Delta pH^* < 1$ (Figure 1). At pH_{min}, 68 °C, the exchange rates are slower than model compound rates by the same factor. The rates for resonances 1, 2, 3, 4, 6, 7, and 9 are 0.074, 0.13, 0.063, 0.069, 0.063, 0.084, and 0.074 h^{-1}. The model compound rates (Molday et al., 1972) based on the assignments of Dubs et al. (1979) at 68 °C and pH_{min} are 10.0, 19.5, 10.10, 10.4, 11.0, 13.9, and 10.4 min^{-1}, respectively. For each resonance at 68 °C and pH_{min}, the ratio between the extrapolated model compound rate and the observed rate is ±9% of 9×10^3.

At 51 °C, the pH*–rate profile obtained between pH* 7.2 and 9.2 shows the same OH^- ion dependence as at 68 °C for resonances 2, 4, 7, and 9. For resonances 1, 3, and 6 at 51.3 °C, the pH*–rate profiles between pH* 7.2 and 10.6 are curved. Further, for resonances 3 and 6, there is a pH*-in-

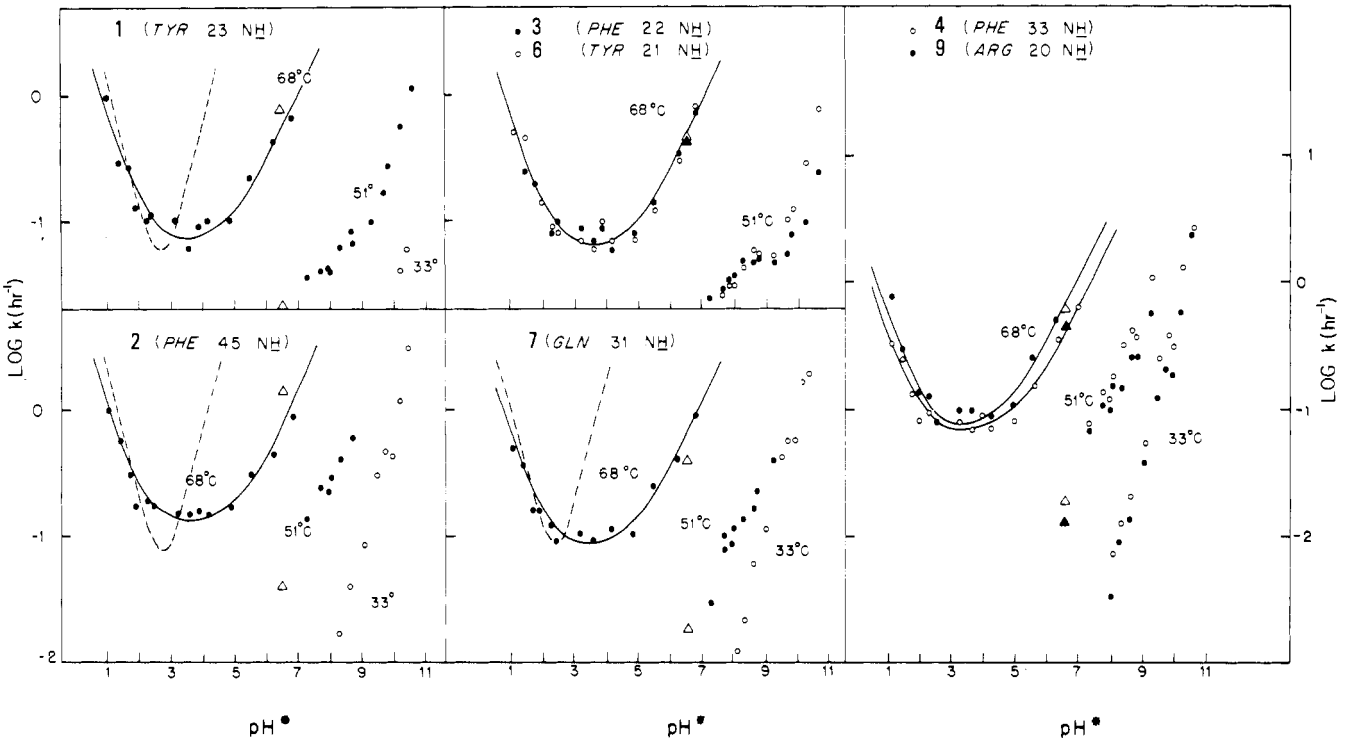

FIGURE 1: pH dependence of exchange rates of single protons in BPTI. The numbers refer to resonances in the NMR spectrum (Hilton & Woodward, 1978). The assignments in parentheses are from Dubs et al. (1979). The circles are data of Hilton and Woodward; triangles are from Wuthrich & Wagner (1979) and Brown et al. (1978) extrapolated from 55 to 51 °C or from 60 to 68 °C by using activation energies determined at pH* 7.7. The solid curves are fits of the pH profile at 68 °C to the equation $k = k_1[H^+]^{0.81} + k_2[H^+]^{-0.51} + k_3$. Dashed lines are calculated model compound rates at 68 °C ($\times 10^{-4}$) from the rules of Molday et al. (1972).

dependent plateau from pH* 8.4 to 9.6 (Figure 1).

At 33 °C, the pH* dependence is clearly different from that at higher temperatures; the data fall on a line with slope $\Delta(\log k)/\Delta pH^* \simeq 1$. The exchange rates at 33 °C were obtained only for resonances 1, 2, 4, 7, and 9 as rates for the other protons fall outside the observation range.

A careful determination of the temperature dependence of the BPTI downfield resonances was carried out between 43 and 68 °C at pH* 7.7. These data are shown together with the rates at 33 °C for four of the resonances extrapolated from the pH-dependence studies in Figure 2. For resonances 1, 3, and 6, for which the 33 °C data are not available, the apparent activation energy is constant within error between 43 and 68 °C. For resonances 4 and 9, the Arrhenius plots are linear from 48 to 68 °C but show curvature at 43 and 33 °C. Resonance 2 has an increasing activation energy at higher temperatures, and resonance 7 shows curvature over the entire temperature range. It is notable that for all but resonance 2 the Arrhenius plots extrapolate to approximately the same value at 68 °C (Figure 2). The apparent activation energies obtained from the linear, high-temperature regions of Figure 2 for resonances 1, 3, 6, 4, and 9 are 57, 65, 65, 46, and 48 kcal/mol (±10%), respectively.

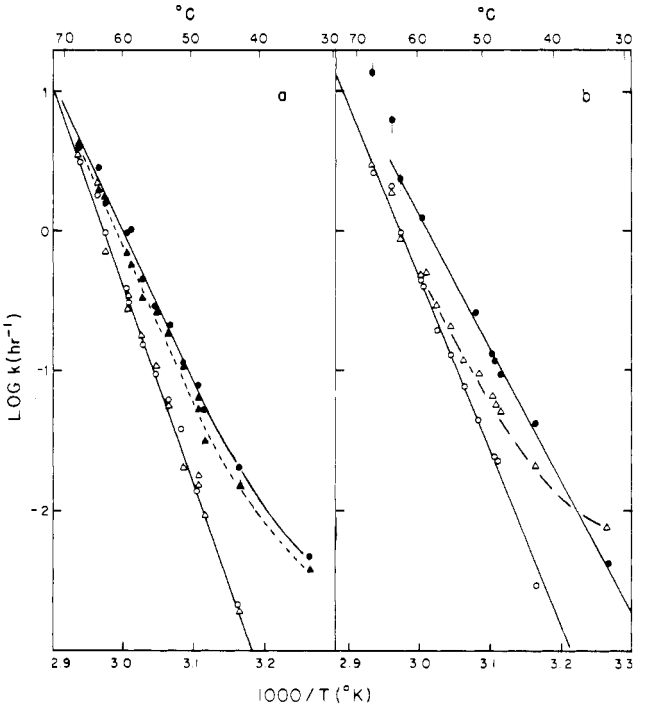

FIGURE 2: Temperature dependence of exchange rates of single protons in BPTI at pH* 7.7. (a) (○) resonance 3; (△) resonance 6; (●) resonance 4; (▲) resonance 9. (b) (○) resonance 1; (●) resonance 2; (△) resonance 7. The points at 33 °C were extrapolated to pH* 7.7 from the pH–rate data at 33 °C in Figures 1 and 4.

Discussion

Several new features of the mechanism of solvent isotope exchange of single protons in BPTI are apparent from analysis of Figures 1 and 2. (1) For each proton there are at least two conformational processes, one of high energy and the other of low energy, that provide accessibility to solvent. (2) The high-energy conformational fluctuation is rate limiting at 51 °C, pH* 8.4–9.6, for the two slowest exchanging resonances, 3 and 6. (3) Assuming the NMR assignments made by Dubs et al. (1979), shown in Figure 3, adjacently hydrogen-bonded β-sheet protons may have closely similar exchange parameters when they are oriented between the same peptide strands, as for resonances 4 (Phe-33 NH) and 9 (Arg-20 NH), or when they are oriented to different peptide strands, as for the resonances 3 (Phe-22 NH) and 6 (Tyr-21 NH).

(1) The data in Figures 1 and 2 demonstrate that there are at least two types of protein motions that determine accessi-

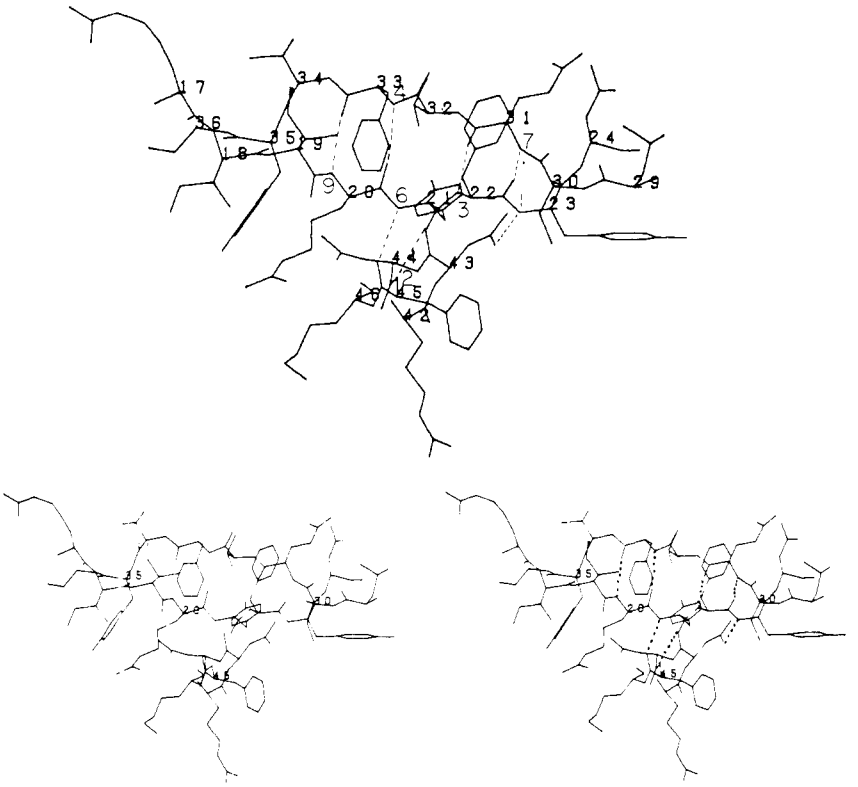

FIGURE 3: Computer projection of the X-ray crystal structure of BPTI showing the β-sheet region containing the exchanging protons. Hydrogen bonds are shown as dashed lines; side chains are labeled by sequence position. Assignments of Dubs et al. (1979) are shown with our resonance numbers next to the amide proton (drawing provided by Dr. Richard J. Feldmann, National Institutes of Health).

bility of these β-sheet protons to solvent; one is evident at higher temperatures, 51–68 °C, and the other is evident at lower temperature, 33 °C. Rates of exchange by the first have a high activation energy and about a half-order dependence on OH^- ion, while rates of exchange by the second have a lower activation energy and a higher order dependence on OH^-.

The Arrhenius plots of exchange rates at pH* 7.7 for resonances 2, 4, 7, and 9 are curved over the range 33–68 °C (Figure 2). Resonances 1, 3, and 6 have rates outside the observation window below 43 °C, and their activation energies are reasonably constant from 43 to 68 °C. Apparent activation energies obtained from the linear, high-temperature regions range from 46 to 65 kcal/mol (see Results); an upper estimate for the activation energy between 33 and 48 °C for the exchange of resonances 4, 7, and 9 is 30 kcal/mol. These data are roughly consistent with the limited data of Richarz et al. (1979), who report average activation energies at pH 8 obtained from linear fits to three to four data points over the range 10–60 °C. These data also supersede our earlier estimates of the activation energies obtained from 58 to 68 °C, pH* 6.85 (Hilton & Woodward, 1978).

The Arrhenius plots are not only curved, they converge at high temperatures. This suggests that the apparent activation energy for each proton rises with increasing temperature due to a shift in the contribution from one or more low-energy processes to a higher activation energy process that is similar for all the protons.

The simplest model to explain the data in Figures 1 and 2 is that there are two discrete types of processes, process a and b, with different activation energies and different pH dependencies, whose relative contributions to the observed exchange will depend on the pH and temperature. We envision each process as involving interconversion between conformational substates. Then, as the temperature is raised at constant pH, the folded conformation shifts from a population of many substates interconverting by low-energy, low-amplitude transitions with little pH dependence to a population of a few substates interconverting by high-energy, high-amplitude, pH-dependent transitions.

For illustration of this idea, hypothetical pH–rate profiles for each type of process for resonance 1 are shown at several temperatures in Figure 4. The curves for process a are constructed from the data at 68 °C (Figure 1) by using the apparent activation energy at high temperature to estimate process a at lower temperatures. The curves for process b are constructed from the 33 °C data by using an activation energy of 30 kcal/mol. The exchange kinetics expected to be observed are indicated by the dashed lines. The data points are from Figure 1 and Wuthrich & Wagner (1979).

These curves predict several aspects of isotope exchange kinetics which can be tested by experiment. First, they predict that at high temperatures and high pH values there will be a shift from the high activation energy process a to the low energy process b at the point of intersection of the curves (Figure 4). Such behavior is observed at 51 °C for the slowest exchanging resonances (1, 3, and 6), for which exchange rates shift to first-order dependence on OH^- at pH >10 (Figure 1). Second, they predict that at lower temperature this shift will take place at lower pH values, specifically at pH $\simeq$8 at 45 °C for resonance 1 (Figure 4). The data of Wuthrich and co-workers fit the predicted curves for resonance 1 remarkedly well (Figure 4).[1] Third, our model predicts that at pH_{min}

[1] The agreement of Wuthrich's 45 °C data is essentially in the shape of the pH–rate profile rather than in the precise value of the exchange rates, as the rates reported for 45 °C overlap our 51 °C data at pH* >9.8 except for resonances 3 and 7. Since the activation energy in the range 51–45 °C is $\geq$20 kcal/mol, the overlap between the 45 and 51 °C rates obtained in the two labs may reflect some differences in the BPTI solution conditions.

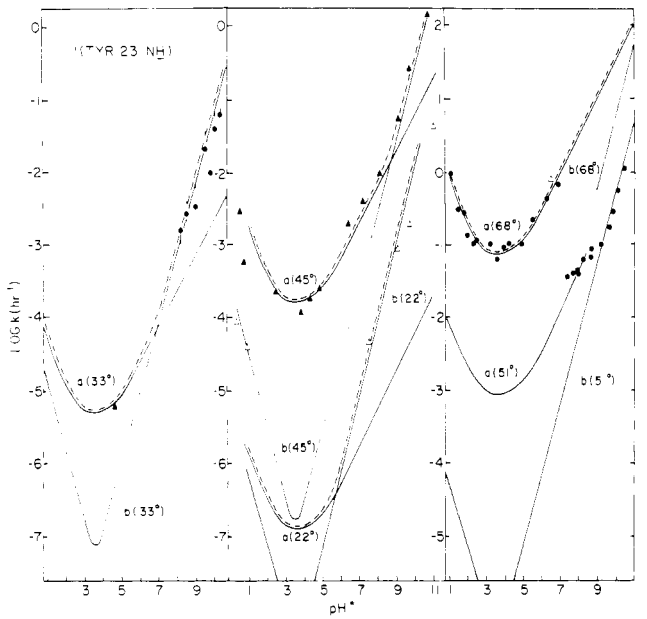

FIGURE 4: Model for the temperature dependence of the pH profile of resonance 1 (Tyr-23 NH) exchange rates. Kinetics for process a or b are shown as solid curves; dashed curves are observed exchange kinetics predicted by the model. Curves for process a are derived from the 68 °C data by using an activation energy of 57 kcal/mol; curves for process b are derived from a straight-line fit to the data at 33 °C and an activation energy of 30 kcal/mol. Circles are data from Hilton and Woodward; triangles are from Wuthrich & Wagner (1979) and Brown et al. (1978). For the latter, the 33 and 68 °C points were extrapolated from 36 and 60 °C data by using an activation energy of 57 kcal/mol.

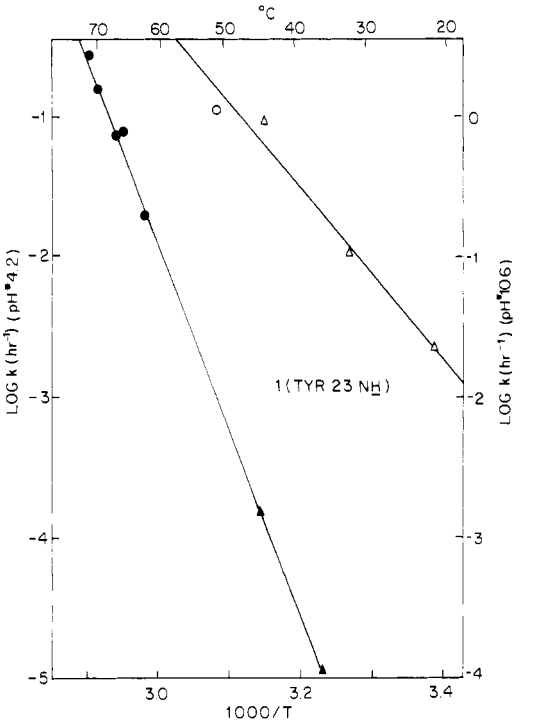

FIGURE 5: Temperature dependence of resonance 1 (Tyr-23 NH) exchange rates at pH* 4.2 (closed symbols) and pH* 10.6 (open symbols). Circles are data from Hilton and Woodward; triangles are from Wuthrich & Wagner (1979) with the pH* 4.2 values extrapolated from data at pH* 4.6 by using the pH dependence at 45 °C. The apparent activation energies are 60 kcal/mol at pH* 4.2 and 28 kcal/mol at pH* 10.6.

process a will dominate, even around room temperature, and the activation energy measured from about 22 to 68 °C at pH_{min} will be constant and $\simeq$60 kcal/mol for these resonances, that at basic pH values process b will dominate and the activation energy will be constant over a broad temperature range at 20–35 kcal/mol, and that at intermediate pH values the Arrhenius plots may be curved. These predictions are realized in the comparison of Figures 2 and 5 and in the activation energies at pH_{min}. Figure 5 shows the temperature dependence for resonance 1 around pH_{min} and at pH* 10.6. Within the error of the sparse data, the activation energy from 36 to 69 °C at pH* 4.2 is linear and 60 kcal/mol, while at pH* 10.6 the activation energy between 22 and 51 °C is linear and 28 kcal/mol. At intermediate pH the activation energy will be a function of the relative contribution of processes a and b; at pH* 7.7, over the range 36–71 °C, resonances that can be observed below 43 °C change to low activation energy at lower temperatures (Figure 2). For resonance 1 at pH* 7.7, the model in Figure 4 predicts that process a will dominate from 45 to 68 °C and therefore that the activation energy should be constant and high in this range; this is observed (Figure 2). At pH_{min}, the Arrhenius plots for resonances 2, 3, 4, 6, and 9 constructed from the same sources as that for resonance 1 (Figure 5) are linear over the range 36–71 °C, pH* 4.2, and have apparent activation energies from a least-squares fit to the data of 51, 65, 63, 62, and 64 kcal/mol, respectively. For resonance 7, the 36 °C rate is not available and the activation energy between 45 and 71 °C is linear and 65 kcal/mol. A single point at 22 °C for resonance 7 at pH* 4.2 shows that the temperature dependence changes to lower activation energy between 22 and 45 °C. The differences between these values of the activation energies at pH* 4.2 previously reported for the interval 62–71 °C (Hilton & Woodward, 1978) arise from the bias of the lowest temperature points, which are on the slow limit for these experiments and have the highest experimental error.

In summary, the complex exchange kinetics of the slowest exchanging protons in BPTI are explained by a simple model of two types of dynamical processes that are different in activation energy. We propose that the low activation energy process b is the general exchange process of interest in the native conformation of globular proteins involving low-energy, small-amplitude fluctuations (Woodward & Rosenberg, 1971a; Woodward, 1977). We propose that process a is a large-amplitude process related to major unfolding. Our model has a precedent in the hydrogen-exchange literature (Woodward et al., 1975a; Ellis et al., 1975) and has no complex ad hoc assumptions. The present model differs from our earlier suggestions for the BPTI exchange mechanism (Hilton & Woodward, 1978).

Process a has characteristics of thermal unfolding, but the high activation energy process cannot be the major cooperative transition if we assume that the kinetics of the transition are the same in the range pH 5–11 as at low pH. BPTI is so stable that the thermal unfolding transition cannot be measured at pH >3.5 (Vincent et al., 1971). At pH 1, 86 °C, the midpoint of the thermal unfolding transition, the interconversion of unexchangeable resonances for the same proton in the native and denatured forms is slow on the NMR time scale (Wuthrich et al., 1978b). Exchange cannot be mediated by this slow a transition since the chemical exchange step would not enter the overall exchange expression and typical acid/base catalysis would not be observed. At pH $\simeq$7, in D_2O or H_2O, the unexchangeable protons in the BPTI spectrum at 85–87 °C show no chemical-shift changes relative to the low-temperature, time-average structure (Masson & Wuthrich, 1973; Wagner et al., 1976). At 87 °C, pH 7, the downfield exchangeable resonances are not observed in D_2O due to rapid

isotope exchange but are observed in H_2O, indicating that the average magnetic environment of these β-sheet protons is intact at temperatures 20 °C higher than those in our experiments (Wagner et al., 1976). Both motional processes indicated by the hydrogen-exchange data then are apparently processes of the folded macrostate. Since few proteins are as stable to heat as BPTI, the high activation energy process may not be general for globular proteins. That the temperature dependence and the pH dependence in the base-catalyzed region for process a are somewhat different for these resonances also suggests that more than one large-amplitude transition is involved, even though at pH_{min}, 68 °C, the exchange rates are slower than model compound rates by the same factor.

Our model explains why the thermal stability of BPTI homologues and derivatives is correlated to the hydrogen exchange rates at pH 4.6, 36 °C (Wagner & Wuthrich, 1979). In the region of the pH_{min}, including pH 4.6, process a dominates the exchange kinetics at temperatures ≥ 36 °C and process a is expected to be correlated to thermal unfolding. At different conditions of pH and temperature, where process b determines the exchange mechanism, our model predicts that the exchange rate is not correlated to thermal stability. In the same vein, we expect that process a will be accelerated by urea and other denaturants while process b will not.

This differs from the interpretation of Wuthrich and coworkers (Wuthrich et al., 1978a; Wagner & Wuthrich, 1978; Richarz et al., 1979). Based on the observation that the thermal stability of BPTI homologues and derivatives is correlated to the hydrogen exchange rates at pH 4.6, 36 °C, while the flip rates of the tyrosine side chains are not, these authors have postulated that the general protein conformational fluctuations governing proton exchange in the range pH 1–11, 10–60 °C, involve opening of hydrogen-bonded secondary structure to give motions of intact hydrophobic domains relative to each other.

With regard to the pH dependence, process a for all the resonances and process b for resonances 3 and 6 are not first order with respect to hydroxyl ion, as expected for simple base catalysis. The explanation of this depends on whether the difference between the observed exchange rates for these protons in native BPTI and their predicted exchange rates in an unordered peptide is due to effects on the chemical exchange step or to pH and temperature effects on conformational processes. Although the answer is not clear, it is useful to review several aspects of the question that arise.

The chemical exchange step for isotopic exchange of peptide amide protons is both acid and base catalyzed [Woodward & Hilton (1979) and references therein]. The slow step is the formation of a charged intermediate by N- or O-protonation in acid catalysis and by extraction of the amide proton in base catalysis. For model compounds, the rate for the chemical exchange step, k_{cx}, is

$$k_{cx} = k_H[H^+] + k_{OH}[OH^-] + k_{H_2O} \quad (1)$$

where k_H, k_{OH}, and k_{H_2O} are the rate constants for acid-catalyzed, base-catalyzed, and direct exchange with water. The latter is negligible for model peptides freely exposed to solvent. The pH–rate profile goes through a minimum at the pH for which the first two terms on the right are equal, pH_{min}. For random conformation peptides, pH_{min} is pH ≃3 and exchange away from the minimum region is first order with respect to hydrogen and hydroxyl ion. In native proteins, pH_{min} is usually but not always pH ≃3 and the base-catalyzed kinetics are often less than first order in OH^- ion.

Since exchange from folded BPTI is acid and base catalyzed, for each proton in the native structure

$$k_n = \beta_H k_{H_n}[H^+]_n + \beta_{OH} k_{(OH)_n}[OH^-]_n + \beta_{H_2O} k_{(H_2O)_n} \quad (2)$$

where k_n is the observed exchange rate, k_{H_n}, $k_{(OH)_n}$, and $k_{(H_2O)_n}$ are rates for acid- and base-catalyzed and direct exchange for that proton in the native conformation of the protein, $[H^+]_n$ and $[OH^-]_n$ are the ion concentrations at the exchange site in the native protein, and β_H, β_{OH}, and β_{H_2O} are the equilibrium probabilities that the proton is accessible for exchange.

If the chemical exchange rate for the proton in the native protein has the same value as for model compounds, then all of the difference between the observed pH and temperature dependence of the exchange kinetics of native proteins, as compared to unfolded peptides, resides in protein conformational processes. Then for base-catalyzed exchange, $k_{(OH)_n}[OH^-]_n \equiv k_{OH}[OH^-] = k_{cx}$ and the conformational parameters can be calculated from the observed exchange rate and model compound values of k_{cx}. Alternatively, there have been suggestions that differences between exchange kinetics of native and unfolded proteins may be due in part to effects on the chemical exchange step; if exchange occurs in the protein matrix, then the chemical exchange term may be different from model compounds in the value of the catalytic rate constant, in the effective OH^- ion activity, or both. Then $k_{(OH)_n}[OH^-]_n \neq k_{OH}[OH^-]$, and conformational parameters calculated from the observed exchange rates and model compound data have no clear physical relevance.

Whether the pH dependence of process a is ascribed to effects on the chemical exchange step or on the conformational process, the explanation must account for why these apparently do not affect process b for four resonances. One possibility is that the motions at low temperature involve low-amplitude fluctuations that in general do not perturb interactions between charged groups. Since the charge-bearing side chains are on the surface and have substantial rotational freedom (Gurd & Rothgeb, 1979), their average electrostatic interactions may not be affected by small internal motions. However, the high-amplitude motions may displace charged surface groups relative to each other. As these experiments are carried out at an ionic strength of 0.3 M, one does not expect electrostatic effects to be important. Nevertheless, some type of interactions that depend on the charge of the protein appears to be the only viable explanation for the high-temperature results.

For process a, pH_{min}^* ≃3.6, ≃0.8 pH unit higher than the pH_{min} calculated for each proton from empirical rules (Figure 1). Again the question is whether this arises from effects on the chemical exchange term or on the protein conformational process. An electrostatic contribution to the effective OH^- ion concentration calculated from the smeared charge model (Linderstrøm-Lang, 1924) would give a pH_{min} lower than that for model compounds. A lower effective K_w would give a higher pH_{min}, as would a greater increase in the acid-catalyzed exchange at 68 °C relative to base-catalyzed exchange (Hilton & Woodward, 1978). The latter now seems to be the most attractive explanation for the pH_{min} of process a, as BPTI is known to be less thermally stable at low pH. The shallowness of the pH_{min} region as compared to model compounds can arise from acid and base terms that are less than first order in H^+ and OH^- ions (Hilton & Woodward, 1978).

(2) The pH*–rate profiles of resonances 3 and 6 plateau between pH* 8.4 and 9.6 (Figure 1); the profile of resonance 1 also levels off around the same pH*, a feature more evident in Figure 4. If as suggested above the exchange at high pH* shifts to process b, then the observed sigmoidal shape of the profile for resonances 3 and 6 in Figure 1 is a combination of a leveling out of process a at pH >8.4 and the entry of process b at pH >10 (Figure 6). We have then to explain

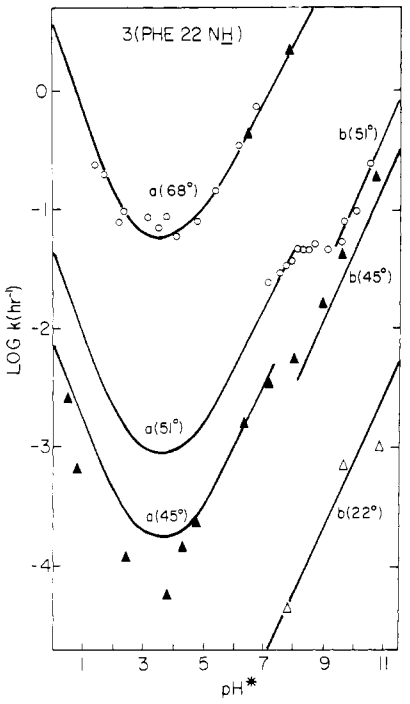

FIGURE 6: Model for the contributions of processes a and b to the pH profile of resonance 3 (Phe-22 NH) exchange rates at 22–68 °C. Solid curves for process a are derived from a fit to the data at 68 °C by using an activation energy of 65 kcal/mol; solid curves for process b are derived from a linear fit to the 51 °C data at pH* >9 and an activation energy of 30 kcal/mol. Circles are data from Hilton and Woodward; triangles are from Wuthrich & Wagner (1979) and Brown et al. (1978). For the latter, the triangles at 68 °C are extrapolated values from data at 60 °C by using an activation energy of 65 kcal/mol.

why for resonances 1, 3, and 6 process a is pH independent at pH >8.4, while other resonances show no evidence of such an effect.

An interesting possibility is that the chemical exchange step at high pH has become very large relative to the protein conformational reactions so that it no longer enters the observed exchange, as in the "EX_1" case in the notation of Hvidt (Hvidt & Neilsen, 1966; Hvidt, 1973). This is consistent with the fact that these are the slowest exchanging amide protons in BPTI. In the EX_1 case the observed exchange rate gives the rate by which conformational transitions provide solvent accessibility for the buried proton.

We can express the sum of the motions for process a between native conformational substates, NH, in which the proton is inaccessible and native conformational substates, NH′, in which the proton is accessible for exchange with deuterium to give ND.

$$\mathrm{NH} \underset{k_2}{\overset{k_1}{\rightleftharpoons}} \mathrm{NH'} \xrightarrow{k_3} \mathrm{ND} \qquad (3)$$

Taking $k_3 = k_{(OH)_n} = k_{cx}$, this is formally equivalent to the scheme of Hvidt; for a buried proton, $k_1 \ll k_2$, and when $k_{cx} \gg k_2$, $k_n \simeq k_1$.

It is also possible that the pH-independent plateau arises from local effects from the titration of an ionizing group. In this pH region a number of groups are titrating; for the N-terminal amino group $pK_a = 8.1$ (Brown et al., 1978), for the four lysine side chains $pK_a = 10.6$–10.8 (Brown et al., 1976), and for the four tyrosine side chains $pK_a = 9.9$–11.1 (Wagner et al., 1976). Deprotonation of the N-terminal amino group could alter its salt bridge with the C-terminal carboxyl (Brown et al., 1978; McCammon et al., 1979), which in turn could affect the protein motions determining the accessibility of these protons.

These alternatives may be differentiated experimentally by the temperature dependence of the pH at which the observed pH–rate curve levels off. If the effect is due to a titration of amino or phenolic groups, at lower temperatures the break should be at higher pH*, as the enthalpy of ionization for these groups is positive. On the other hand, if it is because the conformational transition becomes rate limiting, then at lower temperatures the break in the pH*–rate curve should occur at lower pH* values. This is because the activation energy of $k_{cx} \simeq 20$ kcal/mol is about half the enthalpy of the conformational process and at lower temperatures the same relative values of the conformational accessibility rates and the base-catalyzed chemical exchange rates will be attained at lower pH*.

Comparison of our data for resonances 3 and 6 with the 45 °C data of Wuthrich & Wagner (1979) (Figure 6) suggests that the latter is the case. At 51 °C the pH-independent region is marked; at 45 °C the inflection in the pH–rate profile is present, and it breaks at lower pH. At 45 °C the inflection is less prominent, as our model for the relative contributions of processes a and b predicts. The inflections in the data for resonances 3 and 6 at 45 °C were regarded by the authors as experimental deviation from the linear curve for base catalysis.

Although a more detailed study of the pH dependence as a function of temperature in this region is needed before a firm interpretation can be made, these data support the conclusion that, for process a at high pH, the conformational transitions exposing the protons of resonances 1, 3, and 6 to solvent are limiting and have a rate equal to the observed rate in the pH-independent region. For resonance 3, this is 5.1×10^{-2} h^{-1} at 51 °C and 4.8×10^{-3} h^{-1} at 45 °C.

For resonance 3 (Phe-22 NH), values of k_{cx} (Molday et al., 1972) at the break in the pH–rate profile are 3.9×10^7 h^{-1} at 51 °C, pH* 8.4, and 3.5×10^6 h^{-1} at 45 °C, pH* 7.6. At the break in the pH–rate profile for process a, k_2 is on the order of k_{cx}; this magnitude for k_2 is inconsistent with slow exchange between NH and NH′ NMR signals at the midpoint of the thermal unfolding. The free energy of $K_{eq} = k_1/k_2 \simeq k_n/k_{cx}$ is on the order of 15 kcal/mol at 51 °C for process a.

In principle, k_2 can be calculated for eq 3 at pH values where the chemical exchange rate does contribute to the observed exchange rate and $k_1 + k_2 \gg k_3$. Then

$$k_n \simeq k_1 k_3/(k_1 + k_2) \qquad (4)$$

and k_2 can be determined from the observed exchange rate, k_n, if it is assumed that the apparent pH independence of k_1 continues at lower pH and that $k_3 = k_{cx}$ (Hvidt & Neilsen, 1966). The data presently available are not precise enough to warrant these calculations.

(3) For qualitative examination of the crystal structure in terms of of the hydrogen exchange kinetics and the assignments of these protons, Figure 3 shows a drawing of the relevant region. All of the protons are in β-sheet hydrogen bonds, except resonance 1 (Tyr-23 NH) which is hydrogen bonded to a side-chain carboxyl (Dubs et al., 1979). All correspond to sequences in the rigid core of the protein with the lowest root mean square displacements of the α carbons relative to the average dynamical structure as calculated by McCammon et al. (1977).

As seen in Figure 3, resonances 4 (Phe-33 NH) and 9 (Arg-20 NH), which have very similar hydrogen exchange kinetics at all temperatures and pH values, comprise adjacent hydrogen-bond rungs on the β sheet between the same peptide strands; it seems reasonable that the internal motions that

expose these two protons should be very similar. However, the pair, resonance 3 (Phe-22 NH) and 6 (Tyr-21 NH), which also have the same hydrogen exchange parameters, including the unusual pH independence around pH* 9, are oriented in opposite directions and bonded between two different strands of β sheet. Since Gln-31 NH, assigned to resonance 7, is hydrogen bonded to the carboxyl of Phe-22, and Phe-22 NH, assigned to resonance 3, is hydrogen bonded to the carboxyl of Gln-31, this raises the possibility that resonances 6 and 7 are incorrectly assigned. If the assignments are in fact correct, the protein motions that expose protons hydrogen bonded to different peptide strands have the same pH and temperature dependence and the same rates, while the protein motions that expose two well buried protons comprising adjacent β-sheet hydrogen bonds have quite different pH and temperature dependencies.

References

Bradbury, J., & Brown, L. (1973) *Eur. J. Biochem. 40*, 565.

Brown, L., DeMarco, A., Wagner, G., & Wuthrich, K. (1976) *Eur. J. Biochem. 62*, 103.

Brown, L. R., DeMarco, A., Richarz, R., Wagner, G., & Wuthrich, K. (1978) *Eur. J. Biochem. 88*, 87.

Carter, J. V., Knox, D. G., & Rosenberg, A. (1978) *J. Biol. Chem. 253*, 1947.

Deatherage, J. F., Loe, R. A., Anderson, C. M., & Moffat, K. (1976) *J. Mol. Biol. 104*, 687.

Dubs, A., Wagner, G., & Wuthrich, K. (1979) *Biochim. Biophys. Acta 577*, 177.

Ellis, L. M., Bloomfield, V. A., & Woodward, C. K. (1975) *Biochemistry 14*, 3413.

Englander, S. W. (1975) *Ann. N.Y. Acad. Sci. 244*, 10.

Englander, S. W., & Englander, J. J. (1978) *Methods Enzymol. 49*, 24.

Englander, S. W., Downer, N., & Teitelbaum, H. (1972) *Annu. Rev. Biochem. 41*, 810.

Frauenfelder, H. (1978) *Methods Enzymol. 54*, 506.

Frauenfelder, H., Petsko, G. A., & Tsernoglou, D. (1979) *Nature (London) 280*, 558.

Gelin, B., & Karplus, M. (1975) *Proc. Natl. Acad. Sci. U.S.A. 72*, 2002.

Gelin, B., & Karplus, M. (1977) *Proc. Natl. Acad. Sci. U.S.A. 74*, 801.

Glasoe, P., & Long, F. (1960) *J. Phys. Chem. 64*, 188.

Gurd, F. R. N., & Rothgeb, T. M. (1979) *Adv. Protein Chem.* (in press).

Hilton, B., & Bryant, R. G. (1976) *J. Magn. Reson. 21*, 105.

Hilton, B. D., & Woodward, C. K. (1978) *Biochemistry 17*, 3325.

Huber, R., Kuklas, D., Ruhlman, A., & Steigemann, W. (1971) *Cold Spring Harbor Symp. Quant. Biol. 36*, 141.

Huber, R., Kukla, D., Bode, W., Schwager, P., Bartels, K., Deisenhoffer, J., & Steigemann, W. (1974) *J. Mol. Biol. 89*, 73.

Hvidt, A. (1973) in *Dynamic Aspects of Conformational Changes in Macromolecules* (Sadron, C., Ed.) p 103, Reidel, Dordrecht, The Netherlands.

Hvidt, A., & Nielsen, S. O. (1966) *Adv. Protein Chem. 21*, 287.

Jelinski, L., & Torchia, D. (1979) *J. Mol. Biol. 133*, 45.

Karplus, S., Synder, G., & Sykes, B. (1973) *Biochemistry 12*, 1323.

Knox, D., & Rosenberg, A. (1980) *Biopolymers* (in press).

Lebedev, Y. O., Abaturov, L. V., Pirtskhalava, M. K., & Varshavsky, Y. M. (1976) *Stud. Biophys. 60*, 143.

Linderstrøm-Lang, K. (1924) *C. R. Trav. Lab. Carlsberg 15*, 7.

Linderstrøm-Lang, K. (1958) in *Symposium on Protein Structure* (Neuberg, A., Ed.) p 23, Methuen, London.

Lumry, R. (1978) in *Dynamic Properties of Polyion Systems* (Imai, N., & Sugai, S., Eds.) Kyoto, Japan (in press).

Lumry, R., & Rosenberg, A. (1975) *Colloq. Int. C.N.R.S. No. 246*, 53.

Marinetti, T., Snyder, G., & Sykes, B. (1976) *Biochemistry 15*, 4600.

Masson, A., & Wuthrich, K. (1973) *FEBS Lett. 31*, 114.

McCammon, J., & Karplus, M. (1979) *CRC Crit. Rev. Biochem.* (in press).

McCammon, J., Gelin, B., & Karplus, M. (1977) *Nature (London) 267*, 585.

McCammon, J., Wolynes, P., & Karplus, M. (1979) *Biochemistry 18*, 927.

Molday, R. S., Englander, S. W., & Kallen, R. G. (1972) *Biochemistry 11*, 150.

Munro, I., Pecht, I., & Stryer, L. (1979) *Proc. Natl. Acad. Sci. U.S.A. 76*, 56.

Nakanishi, M., Tsuboi, M., & Ikegami, A. (1973) *J. Mol. Biol. 75*, 673.

Piccinni-Leopardi, C., Fabre, O., & Reisse, J. (1976) *Org. Magn. Reson. 8*, 233.

Richards, F. M. (1979) *Carlsberg Res. Commun. 44*, 47.

Richarz, R., & Wuthrich, K. (1978) *Biochemistry 17*, 2263.

Richarz, R., Sehr, P., Wagner, G., & Wuthrich, K. (1979) *J. Mol. Biol. 130*, 19.

Schoenborn, B. P., Hanson, J. C., Darling, G. D., & Norvell, J. C. (1978) *Acta Crystallogr., Sect. A, Suppl. 4 34A*, 65.

Schreier, A. A., & Baldwin, R. L. (1977) *Biochemistry 16*, 4203.

Tsuboi, M., & Nakanishi, M. (1979) *Adv. Biophys. 12*, 101.

Vincent, J., Chicheportiche, R., & Lazdunski, M. (1971) *Eur. J. Biochem. 23*, 401.

Wagner, G., & Wuthrich, K. (1978) *Nature (London) 275*, 247.

Wagner, G., & Wuthrich, K. (1979) *J. Mol. Biol. 130*, 31.

Wagner, G., DeMarco, A., & Wuthrich, K. (1976) *Biophys. Struct. Mech. 2*, 139.

Weber, G. (1975) *Adv. Protein Chem. 29*, 1.

Woodward, C. K. (1977) *J. Mol. Biol. 111*, 509.

Woodward, C. K., & Rosenberg, A. (1970) *Proc. Natl. Acad. Sci. U.S.A. 66*, 1067.

Woodward, C. K., & Rosenberg, A. (1971a) *J. Biol. Chem. 246*, 4105.

Woodward, C. K., & Rosenberg, A. (1971b) *J. Biol. Chem. 246*, 4114.

Woodward, C. K., & Ellis, L. M. (1975) *Biochemistry 14*, 3419.

Woodward, C. K., & Hilton, B. D. (1979) *Annu. Rev. Biophys. Bioeng. 8*, 99.

Woodward, C. K., Ellis, L. M., & Rosenberg, A. (1975a) *J. Biol. Chem. 250*, 432.

Woodward, C. K., Ellis, L. M., & Rosenberg, A. (1975b) *J. Biol. Chem. 250*, 440.

Wuthrich, K., & Wagner, G. (1979) *J. Mol. Biol. 130*, 1.

Wuthrich, K., Wagner, G., & Bundi, A. (1978a) in *Nuclear Magnetic Resonance in Molecular Biology* (Pullman, B., Ed.) p 201, Reidel, Dordrecht, The Netherlands.

Wuthrich, K., Wagner, G., Richarz, R., & Perkins, S. (1978b) *Biochemistry 17*, 2253.